Molecular Plant Pathology

WILEY

Molecular Plant Pathology

ORIGINAL ARTICLE OPEN ACCESS

Potato Type I Protease Inhibitor Mediates Host Defence Against Potato Virus X Infection by Interacting With a Viral RNA Silencing Suppressor

Minjie Shen[1] | Yonghao Wang[1] | Yi Chen[1] | Jiejun Peng[1] | Guanwei Wu[1] | Shaofei Rao[1] | Jian Wu[1] | Hongying Zheng[1] | Jianping Chen[1] | Fei Yan[1] | Yuwen Lu[1] | Gentu Wu[2]

[1]State Key Laboratory for Quality and Safety of Agro-Products, Key Laboratory of Biotechnology in Plant Protection of MARA, Zhejiang Key Laboratory of Green Plant Protection, Institute of Plant Virology, Ningbo University, Ningbo, China | [2]Chongqing Key Laboratory of Plant Disease Biology, College of Plant Protection, Southwest University, Chongqing, China

Correspondence: Yuwen Lu (luyuwen@nbu.edu.cn) | Gentu Wu (wugentu6066@swu.edu.cn)

Received: 15 January 2025 | **Revised:** 27 February 2025 | **Accepted:** 27 February 2025

Funding: This study was supported by the National Natural Science Foundation of China (32270144), State Key Laboratory for Managing Biotic and Chemical Threats to the Quality and Safety of Agro-products (2021DG700024-KF202425), the Natural Science Foundation of Ningbo City (2022J069), the Natural Science Foundation of Zhejiang Province (LY22C140001) and the K. C. Wong Magna Fund in Ningbo University.

Keywords: P25 | potato type I protease inhibitor | potato virus X | viral RNA silencing suppressor

ABSTRACT

Counteracting plant RNA silencing ensures successful viral infection. The P25 protein encoded by potato virus X (PVX) is a multifunctional protein that acts as a viral RNA silencing suppressor (VSR). In this study, we screened out a potato type I protease inhibitor (PI) in *Nicotiana benthamiana* (NbPI) that interacts with P25. Silencing of *NbPI* by tobacco rattle virus (TRV)-mediated virus-induced gene silencing (VIGS) promoted the infection of PVX. Overexpression of NbPI in transgenic plants conferred resistance to PVX infection. Moreover, transient expression of NbPI impaired the VSR activity and cell-to-cell movement complementation ability of P25. Further experiments showed that P25 protein degradation was through the combination of autophagy and the ubiquitin-26S proteasome system (UPS), leading to impairment of P25. Taken together, we have identified NbPI as a new host factor that compromises PVX infection by targeting and degrading the VSR P25.

1 | Introduction

RNA silencing is one of the main mechanisms by which plants defend themselves from pathogens, including viruses (Ding et al. 2004; Voinnet 2001; Wang and Metzlaff 2005). However, plant viruses have counterdefence virus proteins, known as RNA silencing virus suppressors (VSRs), that counteract this defence mechanism and ensure successful systemic infection in the plant (Baulcombe 2002; Ding et al. 2004; Qu and Morris 2005). One way that VSRs function is by binding to long double-stranded RNA (dsRNA) or small interfering RNA (siRNA) duplexes, subsequently inhibiting siRNA biogenesis or RNA-induced silencing complex (RISC) formation (Lakatos et al. 2006). Another way is by binding to components of the RNA silencing machinery and inhibiting their normal function (Lakatos et al. 2006). The earliest identified VSR protein was 2b of cucumber mosaic virus (CMV; *Cucumovirus CMV*), which has a dsRNA binding domain and an AGO interaction domain (Duan et al. 2012). The P19 protein of tomato bushy stunt virus (TBSV; *Tombusvirus lycopersici*) acts as a VSR by binding to 21-nucleotide (nt) siRNAs, helping viral infection of host plants (Jiang, Lu, et al. 2021; Jiang, Zheng, et al. 2021; Li et al. 2019). Plants have various countermeasures to such attacks from plant viruses. For example, autophagy in plants targets and degrades several VSRs, such as CMV 2b (Diaz-Pendon et al. 2007), rice stripe virus (RSV; *Tenuivirus oryzaclavatae*) P3

(Jiang, Lu, et al. 2021; Jiang, Zheng, et al. 2021) and brassica yellows virus (BrYV; *Polerovirus TUYV*) P0 (Li et al. 2019). Recent reports have identified a protein arginine methyltransferase 6 (PRMT6) that methylates the key arginine residue of TBSV P19 to inhibit its dimerisation and small RNA binding activity (Zhu et al. 2024).

Potato virus X (PVX; *Potexvirus ecspotati*, family *Alphaflexiviridae*) has a single-stranded (ss)RNA genome that encodes five proteins, of which the three triple gene block (TGB) proteins and coat protein (CP) are all involved in viral cell-to-cell and systemic movement (Verchot 2022). TGBp1 (P25) is a multifunctional protein that is also a decisive factor in PVX pathogenicity (Verchot 2022; Wu et al. 2019). P25 has RNA helicase activity (Atabekov et al. 2007) and ATPase activity (Leshchiner et al. 2006). Furthermore, it plays a crucial role in suppressing host RNA silencing (Voinnet et al. 2000) and facilitating the systemic movement of PVX through its interaction with TGBp2/3 (Tilsner et al. 2012). Furthermore, the P25 protein has been reported to interact with Argonaute1 (AGO1) and to mediate the degradation of AGO1 via the proteasome pathway (Chiu et al. 2010). P25 can target chloroplast protein ferredoxin 1 (FD1), interfere with the accumulation of callose mediated by plant hormones, and promote the infection of PVX (Yang, Lu, et al. 2020).

Protease inhibitors (PIs) are a large and complex group of inhibitors that play various roles in development and metabolism by binding to proteases and controlling their activity (Mitsumori et al. 1994; Grudkowska and Zagdańska 2004; Sin et al. 2006; Sawano et al. 2008). Many studies have shown that mechanical damage and chewing by herbivorous insects cause the accumulation of PIs in plants, while the expression of PIs is regulated by plant hormones such as jasmonic acid (JA), ethylene (ET), and abscisic acid (ABA) (Tamayo et al. 2000). PIs can inhibit the activity of protease enzymes produced by fungi and bacteria in the apoplast and play a defensive role in plants by fighting against pathogen infections (Kim et al. 2005; Kim et al. 2006; Sels et al. 2008; Tsybina et al. 2001). There are also several reports that endogenous PIs may provide resistance to plant viruses. The constitutive expression of rice cysteine proteinase inhibitors in tobacco has been found to be potentially associated with resistance to tobacco etch virus (TEV; *Potyvirus nicotianainsculpentis*) and potato virus Y (PVY; *Potyvirus yituberosi*) (Gutierrez-Campos et al. 1999). Additionally, recent findings have shown that StAPI5 in potato (*Solanum tuberosum*) has the potential to defend against multiple virus infections, acting against both PVY and potato virus A (*Potyvirus atuberosi*) (Osmani et al. 2022). Furthermore, the CmPI identified from *Cucumis metuliferus* plays an important role in resistance to potato virus infection in *C. metuliferus* and *Nicotiana benthamiana* (Lin et al. 2015).

Here, we found that a potato type I protease inhibitor in *N. benthamiana*, named NbPI, interacted with PVX P25. In the *NbPI*-silenced plants, infection by PVX resulted in serious viral symptoms and greater accumulation of viral RNAs. Plants overexpressing NbPI had compromised symptoms of PVX infection. Further studies demonstrated that the expression of NbPI induced degradation of P25 and suppressed the function of P25 as a suppressor of RNA silencing. Taken together, these results demonstrate a strategy in which NbPI participates in viral defence against PVX infection by targeting the VSR.

2 | Results

2.1 | PVX P25 Interacts With a Potato Type I Protease Inhibitor

PVX P25 is multifunctional, acting as a suppressor of plant RNA silencing and playing a significant role in viral movement (Voinnet et al. 2000; Bayne et al. 2005). Here, by using yeast two-hybrid assays, we identified an *N. benthamiana* protein interacting with P25 (Figure 1A). The complete nucleotide sequence of the protein was cloned, and BLAST showed that it encoded a potato type I protease inhibitor in *N. benthamiana* (NbPI). To verify the interaction between P25 and NbPI, a bimolecular fluorescence complementation (BiFC) assay and co-immunoprecipitation (Co-IP) experiments were then performed. We cloned the *NbPI* gene into the split-YFP vector pCV-nYFP-C and *P25* into pCV-cYFP-C, then transiently expressed them in *N. benthamiana* plants. Co-expression of NbPI-nYFP and P25-cYFP produced YFP fluorescence at 2 days post-infiltration (dpi), confirming an interaction between these two proteins, whereas co-expression of NbPI-nYFP with a control GUS-cYFP did not (Figure 1B). In a Co-IP assay, plasmids encoding *NbPI*-Myc (C-terminal Myc tag) and *P25*-GFP (C-terminal GFP tag) were transiently expressed in *N. benthamiana* plants, with GUS^{600}-Myc (β-glucuronidase gene with a size of 600 bp, GUS) used as a noninteracting (negative) control. Leaf lysates were immunoprecipitated with anti-Myc beads, and any coprecipitated protein was detected using an anti-GFP antibody (Figure 1C). These experimental outcomes all suggest that NbPI interacts with P25.

2.2 | Overexpression of NbPI Alleviates PVX Infection

Virus-induced gene silencing (VIGS) is a potent approach for studying the loss-of-function of plant genes. The system based on the TRV vector has been well developed and extensively applied (Velásquez et al. 2009). Silencing of the endogenous phytoene desaturase (*PDS*) gene with photobleaching symptoms is used as a control. We therefore used this system to investigate the role of *NbPI* in PVX infection. At 10 dpi of TRV:*PDS*, the systemic (newly emerged) leaf showed a marked leaf bleaching phenomenon (Figure S1A). There was no difference in phenotype between the *NbPI*-silenced and the control plants (Figure S1B), and reverse transcription-quantitative PCR (RT-qPCR) results showed that the expression level of *NbPI* was significantly reduced, indicating that *NbPI* had been silenced successfully (Figure S1C). When *NbPI* silencing was established by TRV:*NbPI* at 10 dpi, PVX-GFP was inoculated onto the plants, and GFP fluorescence was monitored. GFP fluorescence appeared on the systemic leaves of both *NbPI*-silenced and non-silenced plants at 6 dpi, but the intensity of fluorescence was greater in the *NbPI*-silenced plants (Figure 2A). Additionally, the accumulation of PVX CP was greater at both the protein and RNA levels in the plants with silenced *NbPI* compared to the control plants

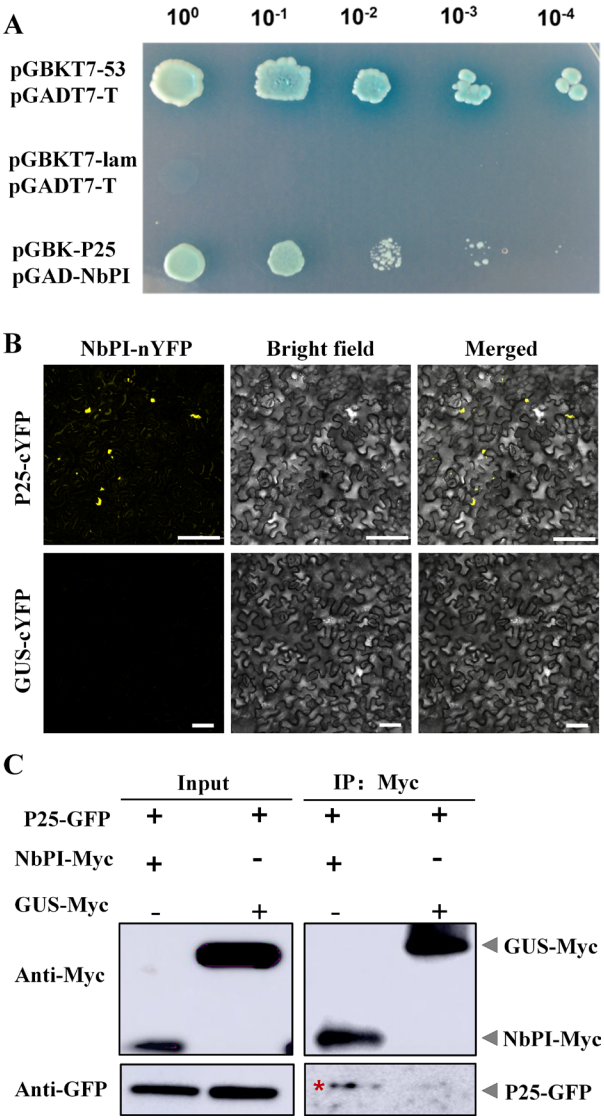

FIGURE 1 | PVX P25 interacts with a potato type I protease inhibitor. (A) Using nuclear yeast two-hybrid analysis, it was confirmed that P25 interacts with NbPI. (B) In order to confirm the interaction between NbPI and PVX P25 in *Nicotiana benthamiana* leaves, bimolecular fluorescence complementation assay was conducted in *N. benthamiana*. Photographs were taken 2 days after *Agrobacterium* infiltration. The YFP region, bright field, and their overlay are shown. Scale bar = 100 μm. (C) The results of co-immunoprecipitation analysis show that NbPI can interact with PVX P25 to form a complex in *N. benthamiana* cells. Different cell lysates were immunoprecipitated with anti-Myc magnetic beads, separated by SDS-PAGE, and detected by anti-Myc monoclonal antibody or anti-GFP monoclonal antibody by western blot.

(Figure 2B,C). Taken together, these findings suggest that silencing of *NbPI* enhances the susceptibility of *N. benthamiana* to PVX infection.

The higher accumulation of PVX in *NbPI*-silenced plants led us to postulate that NbPI might play a defensive role during PVX infection. To test the hypothesis, we first transiently overexpressed NbPI and then inoculated the plants with PVX. The fluorescence of PVX-GFP in the patch with the overexpression of NbPI was weaker than that in the control (Figure S2A). Western blotting revealed that the accumulation of CP was decreased in the patches transiently expressing NbPI (Figure S2B).

To further validate the effect of overexpressing NbPI on PVX infection, the leaf disc transformation method was employed to obtain transgenic tobacco lines expressing NbPI-RFP (C-terminal RFP tag). Through confocal microscopy observation of RFP fluorescence in transgenic progeny of each line, three homozygous lines (1/3/26#NbPI-OE) were identified (Figure S3A,B). Agrobacteria harbouring PVX-GFP were infiltrated onto similar-sized patches of leaves of either the transgenic plants overexpressing NbPI or wild-type plants (control) at 3 weeks of age. At 6 dpi, the GFP fluorescence intensity on the systemic leaves of the *NbPI*-overexpressing plants was significantly lower than that of the wild-type *N. benthamiana* plants (Figure 2D,E). Western blotting results also showed that the accumulation of PVX CP and P25 in plants overexpressing *NbPI* was less than that in the control plants (Figure 2F). Furthermore, the results of RT-qPCR indicated that there was less virus RNA in the systemic leaves of NbPI-OE(s) lines than in the control plants (Figure 2G). At the same time, RT-qPCR analysis confirmed that these three plant lines were overexpressing *NbPI* (Figure S4). This further confirms that NbPI plays a defensive role in PVX infection, and that overexpression of *NbPI* in *N. benthamiana* plants compromised PVX infection.

2.3 | NbPI Affects the Function of PVX P25

To investigate whether the defensive role of NbPI results from impairing the VSR function of P25, GFP-expressing transgenic *N. benthamiana* (16c) plants were used to analyse the effect of NbPI on the function of P25 as a suppressor. 16c plants were infiltrated with agrobacteria expressing GFP to increase the expression of GFP but then initiate post-transcriptional gene silencing to subsequently degrade GFP mRNAs and abolish GFP fluorescence. The leaves of 16c plants were also infiltrated with agrobacteria expressing PVX P25 with NbPI-RFP (C-terminal RFP tag) or Mock-RFP (Figure 3A). At 5 dpi, green fluorescence was almost absent in patches without NbPI, appearing as a red rim, showing that silencing of the GFP gene had occurred (Figure 3A). Patches co-expressing NbPI-RFP, P25, and mGFP were still green, but the GFP fluorescence was weaker than in the positive control (Mock-RFP, P25 and mGFP) (Figure 3A). The supplementary experiments showed that NbPI had no effect on mGFP accumulation (Figure S5). In the patches expressing NbPI, the accumulation of GFP was decreased compared with the positive control, showing that the expression of NbPI impaired the function of P25 as a VSR (Figure 3B).

In addition to being a suppressor of RNA silencing, P25 also acts together with the other TGBs (TGBp2 and TGBp3) as a movement protein for PVX cell-to-cell movement and systemic movement (Verchot-Lubicz et al. 2007). Because we had shown that the expression of NbPI impaired the suppressor function of P25, we then examined whether the expression of NbPI affects the movement function of P25, using PVXΔP25-GFP to analyse the effect of NbPI on the ability of P25 to recover movement-deficient

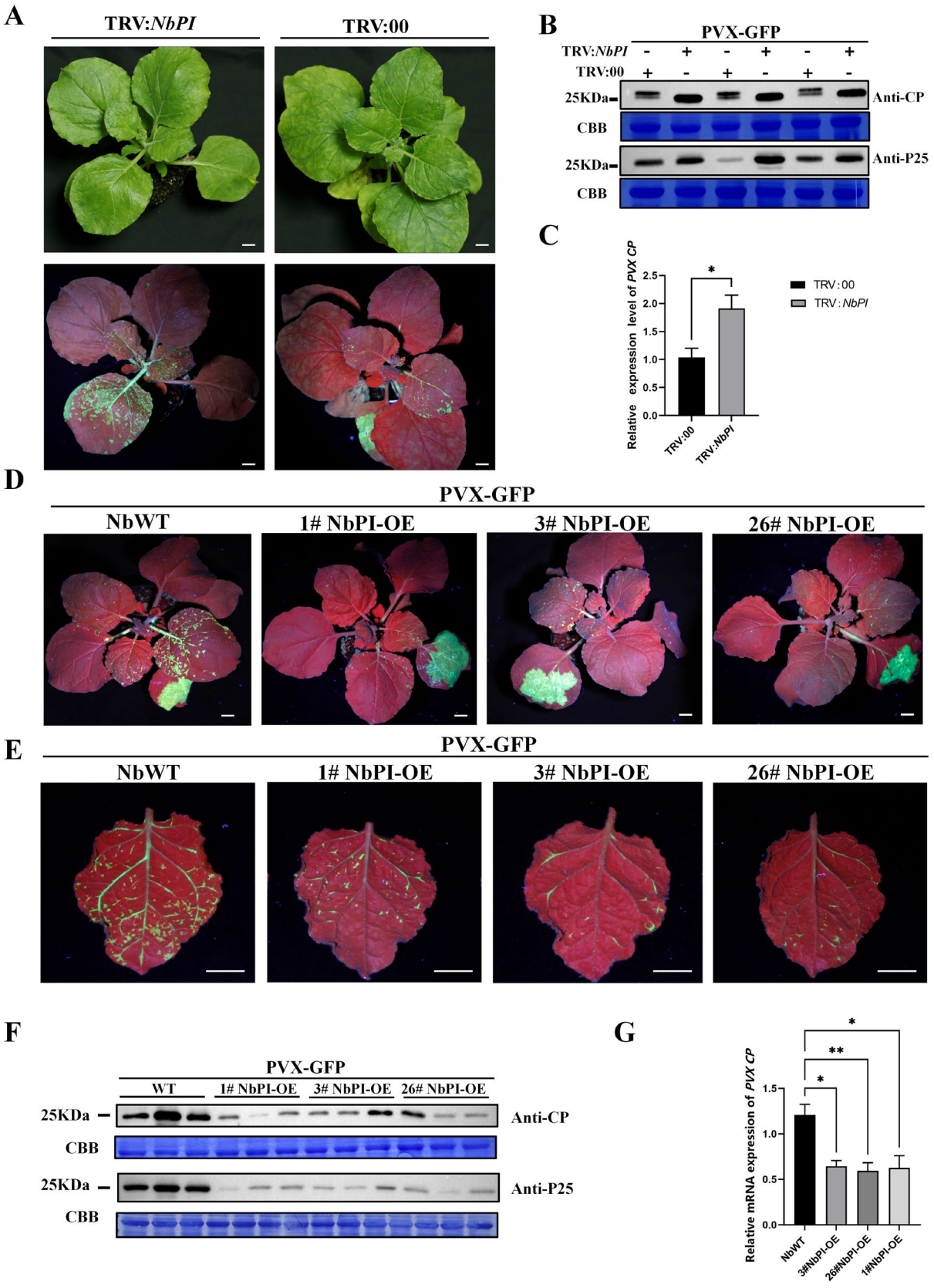

FIGURE 2 | Legend on next page.

PVX. We co-infiltrated PVXΔP25-GFP, P25 with NbPI-RFP or Mock-RFP into different regions of *N. benthamiana* leaves via *Agrobacterium* infiltration. At 4 dpi, the GFP fluorescence intensity and density in the experimental group (NbPI-RFP) were significantly weaker than those in the control group (Mock-RFP), a phenomenon observable under a handheld UV lamp (Figure 3C). Similarly, confocal microscopy revealed that GFP fluorescence was widely distributed in many cells in the control

FIGURE 2 | Overexpression of NbPI alleviates PVX infection. (A) The GFP fluorescence phenotypes of the systemic leaves at 6 days post-inoculation (dpi) after PVX-GFP infection were analysed under natural light and ultraviolet light. Scale bar = 1 cm. (B) Western blot analysis showing the accumulation levels of PVX coat protein (CP) and P25 proteins in the systemic leaves at 6 dpi after PVX-GFP infection. (C) Reverse transcription-quantitative PCR (RT-qPCR) analysis showing the PVX RNA levels in the systemic leaves at 6 dpi after PVX-GFP infection. *Actin II* was used as an internal control. Statistical analysis was conducted using the *t* test (*$p < 0.05$). (D) and (E) GFP fluorescence of systemic leaves in transgenic plants overexpressing NbPI and wild-type *Nicotiana benthamiana* plants after infiltration with PVX-GFP at 6 dpi. Scale bar = 1 cm. (F) Western blot results showing the accumulation of PVX CP and P25 in systemic leaves of the wild-type and transgenic plants overexpressing NbPI in (D) and (E). (G) RT-qPCR analysis showing the PVX RNA levels in systemic leaves of the wild-type and transgenic plants overexpressing NbPI in (D) and (E). *Actin II* was used as an internal control. Statistical analysis was conducted using the *t* test (*$p < 0.05$, **$p < 0.01$).

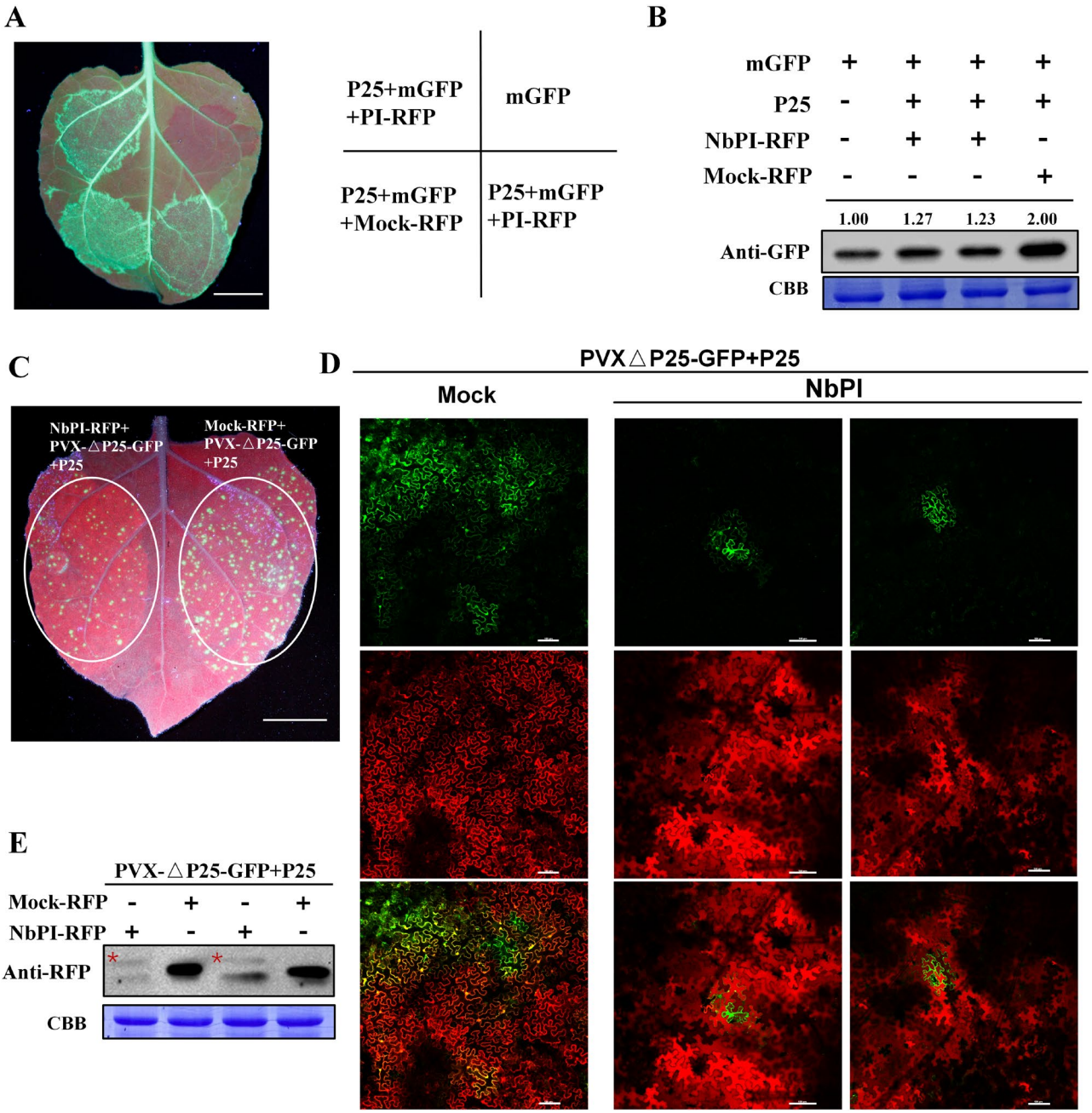

FIGURE 3 | NbPI affected the function of PVX P25. (A) mGFP was expressed alone or in combination with P25 on transgenic *Nicotiana benthamiana* 16c, and the plants were co-infiltrated with Mock-RFP or NbPI-RFP. The GFP fluorescence phenotype of the plants was observed under a handheld UV lamp at 6 days post-infiltration (dpi). Scale bar = 1 cm. (B) Total proteins were extracted from leaves of the same size in the four regions of (A), and the protein accumulation level of mGFP was analysed. (C) PVXΔP25-GFP and P25 were co-infiltrated with Mock-RFP or NbPI-RFP. The GFP fluorescence phenotype of the plants was observed under a handheld UV lamp at 3 dpi. Scale bar = 1 cm. (D) Confocal microscopy images in (C) illustrate the distribution and accumulation patterns of GFP fluorescence, RFP fluorescence and their merged fluorescence. Scale bar = 100 μm. (E) Western blot assay of the expression of NbPI-RFP and Mock-RFP.

group, while in the experimental group, GFP fluorescence was restricted to a few cells (Figure 3D). Confocal microscopy and western blot assays confirmed the expression of NbPI-RFP and Mock-RFP (Figure 3D,E). These results were consistent with the observations under UV light and indicate that NbPI interferes with the normal movement function of P25.

2.4 | NbPI Participates in the Degradation of PVX P25

To further investigate how NbPI affects the function of P25, we co-infiltrated P25-GFP with NbPI-RFP or Mock-RFP (control) and monitored the subcellular localisation and intensity of fluorescence. At 60 h after infiltration, confocal fluorescence observation showed that when P25-GFP and NbPI-RFP were co-expressed, the fluorescence of GFP was significantly less than that of the control group (Figure 4A). Western blotting showed that significantly less P25 accumulated in the NbPI group than in the control group (Figure 4B).

Autophagy and the UPS are the main protein degradation pathways in eukaryotic cells (Varshavsky 2017). To investigate which pathway was involved in the degradation of P25 by NbPI, we co-expressed the P25-GFP and NbPI-RFP for 48 hpi and then added cycloheximide (CHX, a protein synthesis inhibitor) along with 3-methyladenine (3-MA, an inhibitor of autophagy) or MG132 (an inhibitor of the 26S proteasome pathway). Through confocal observation, we found that when NbPI and P25 were treated with 3-MA or MG132 alone, the GFP fluorescence intensity of P25 was not affected compared with the control group (Figure S6A,C). Western blot analysis of P25 protein accumulation showed no significant difference between 3-MA or MG132 treatment alone, but compared with the control group (Mock-RFP), the accumulation of P25 protein was significantly reduced (Figure S6B,D). Previous studies have shown that when the proteasome is inhibited by chemical or genetic defects, autophagy can affect the degradation pathway of the 26S proteasome and remove excessive or damaged proteasomes (Marshall et al. 2021), indicating that the UPS and autophagy can complement each other to manage the nutrient cycle and alleviate protein toxic stress. Therefore, we decided to combine the 3-MA and MG132 treatments and then detect the accumulation of P25 protein co-expressed with NbPI-RFP or Mock-RFP in the same leaf. Compared with the control group (the co-expression group of NbPI and P25 treated only with CHX), the experimental group (the co-expression group of NbPI and P25 treated with CHX, 3-MA and MG132 simultaneously) showed a significant increase in the GFP fluorescence of P25 and a greater accumulation of the protein (Figure 4C,D). The treatment of MG132 plus 3-MA did not significantly affect the P25 fluorescence intensity and protein accumulation in the Mock-RFP group, but these were significantly greater than those in the NbPI-RFP group (Figure 4C,D). In conclusion, NbPI may inhibit the accumulation of P25 through the combination of autophagy and UPS, thereby affecting the important role of P25 in the PVX infection process.

3 | Discussion

PIs play a crucial role in various biochemical processes by specifically binding to proteases and modulating their activities and thus have multiple roles in plant development, metabolism, and pest resistance (Tamayo et al. 2000; Mitsumori et al. 1994; Grudkowska and Zagdańska 2004). PIs have been extensively studied for their significant role as natural insecticides in plants (Zhu-Salzman and Zeng 2015). They inhibit the proteases secreted by insects, thereby preventing insects from obtaining essential amino acids, and directly or indirectly cause the death of insects or difficulties in their development and reproduction (Premachandran et al. 2021). PIs also play a role in combating plant viruses. The expression of rice cysteine protease inhibitor in tobacco provides potential resistance to both TEV and PVY (Gutierrez-Campos et al. 1999). In addition, StAPI5 (identified in potato) and CmPI (identified in *C. metuliferus*) both have resistance effects against multiple potato viruses (Osmani et al. 2022; Lin et al. 2015). Here, the NbPI identified in our study as a potato type I protease inhibitor has also been confirmed to provide resistance to PVX infection. NbPI not only interacts with the P25 protein of PVX but also inhibits its function as a viral silencing suppressor. Mutation analysis has demonstrated that the suppressor function of P25 is necessary for its movement function in a previous study (Bayne et al. 2005). Hence, this also restricts the movement of PVX between cells, consistent with the fact that PVX movement between cells depends on interference with plant RNAs.

The autophagy and UPS, which are responsible for the quality control and degradation of target proteins, jointly regulate the internal homeostasis of eukaryotic cells (Yu and Hua 2023). The two processes are interconnected and can to some extent compensate for each other's functions (Raffeiner et al. 2023). In addition, both autophagy and UPS play crucial roles in plant antiviral defence by degrading viral proteins (Jiang, Lu, et al. 2021; Haxim et al. 2017; Vogel et al. 2007). In our study, co-expression of PVX P25 with *Agrobacterium* harbouring pCV-NbPI-RFP resulted in a significant reduction in the accumulation of PVX P25 protein. However, western blot analysis revealed that co-expression of pCV-P25-GFP and pCV-NbPI-RFP using *Agrobacterium* did not alter the accumulation of P25 protein upon treatment with either MG132 or 3-MA. When autophagy inhibitors and proteasome inhibitors were applied simultaneously, the accumulation of P25 protein was increased in the presence of NbPI, indicating the involvement of both autophagy and the UPS. In a previous study, the effect of NbALY916 on the accumulation of P25 was also through both autophagy and the UPS (Yang, Tian, et al. 2020). This suggests that the degradation of P25 induced by host factors is mediated by autophagy and ubiquitin-proteasome pathways, either directly or indirectly. Thus, NbPI participates in plant defence against PVX by mediating the degradation of P25, although the precise mechanism by which this degradation occurs requires further investigation.

4 | Experimental Procedures

4.1 | Plant Materials and Growth Conditions

Wild-type *N. benthamiana* and transgenic lines expressing green fluorescent protein (GFP) (line 16c) or NbPIOE were grown in pots under constant 60% relative humidity and a 16 h:8 h light:dark photoperiod. To achieve the transgenic overexpression of the *NbPI* gene, the full-length gene of *NbPI*

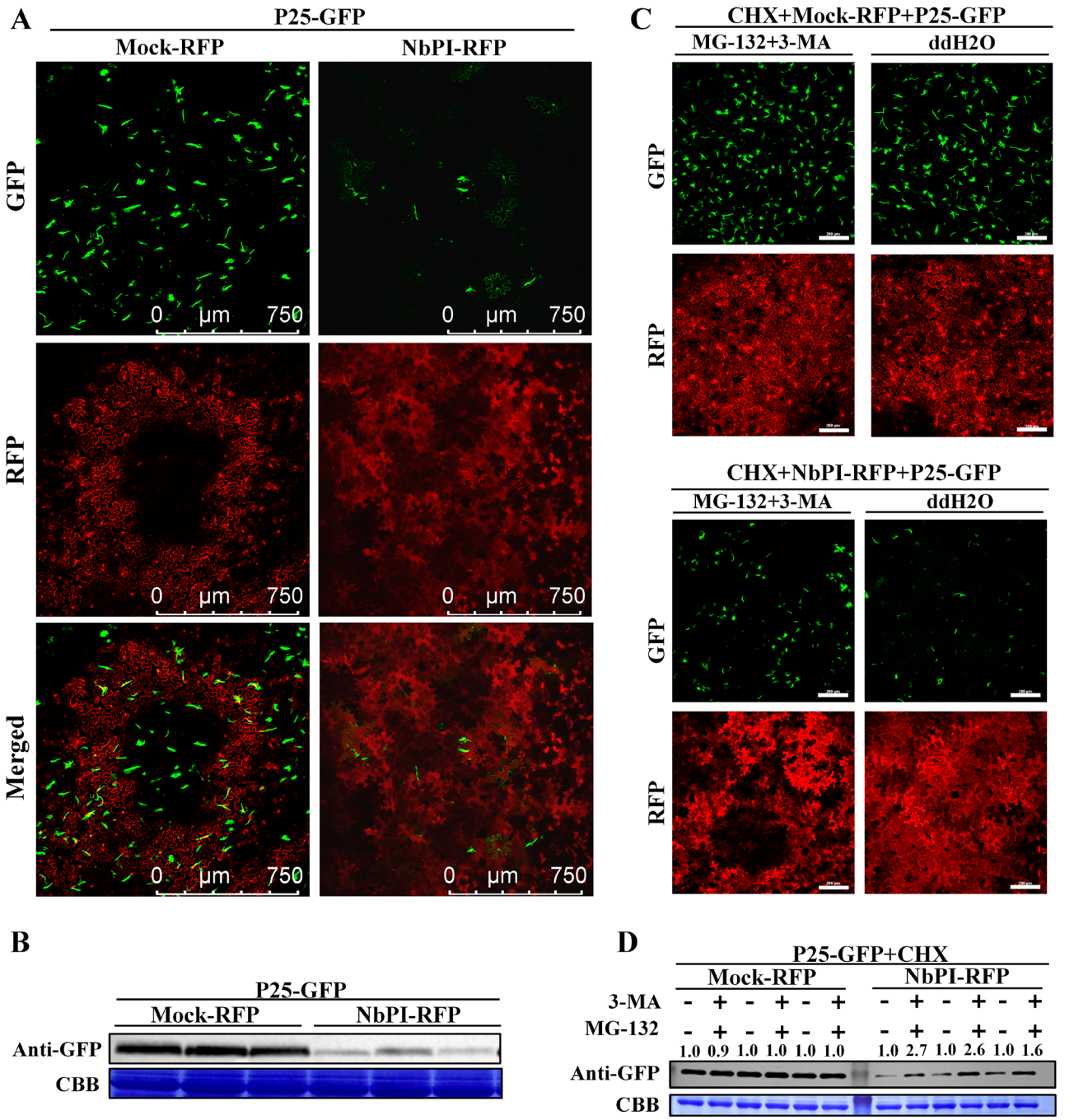

FIGURE 4 | NbPI participates in the degradation of PVX P25. (A) Confocal microscopy images of *Nicotiana benthamiana* leaves co-infiltrated with P25-GFP and either Mock-RFP or NbPI-RFP. Images were captured at 60 h after co-infiltration (hpi). The images show the GFP region, the RFP region, and their overlay. Scale bar = 750 μm. (B) Western blot analysis of the accumulation level of P25 protein in (A). (C) Upper panel: Transient expression of Mock-RFP and P25-GFP in two regions of the same leaf at 48 hpi, followed by treatment with cycloheximide (CHX), MG132 and 3-methyladenine (3-MA) in the experimental group and treatment with CHX alone in the control group at 9 hpi. Confocal microscopy images at 9 hpi. Lower panel: Transient expression of NbPI-RFP and P25-GFP in two regions of the same leaf at 48 hpi, followed by treatment with CHX, MG132 and 3-MA in the experimental group and treatment with CHX alone in the control group at 9 hpi. Confocal microscopy images at 9 hpi. The images show the GFP region and the RFP region. Scale bar = 200 μm. (D) Western blot analysis of the accumulation level of P25 protein in (C).

was cloned into the pCV vector (Lu et al. 2011). Subsequently, *Agrobacterium*-mediated transformation of *N. benthamiana* plants was conducted following a standard protocol (Horsch et al. 1985). The RFP (543/593–636 nm) fluorescence signal in transgenic progeny overexpressing NbPI was observed under an A1R HD25 confocal microscope (Nikon) and confirmed as a homozygous line.

4.2 | Plasmid Construction

The gene sequence was amplified via PCR using KOD FX neo DNA polymerase (Toyobo) (primers are listed in Table S1). Ligation-independent cloning (LIC) technology was used to construct all expression vectors for plant research (Wendrich et al. 2015). The full-length sequence of PVX P25 was obtained from PVX-infected

N. benthamiana cDNA clones, while the full-length sequence of *NbPI* was obtained from *N. benthamiana* cDNA clones. For yeast two-hybrid analysis, the genes were ligated to pGBKT7 and pGADT7 to generate pGBK-P25 and pGAD-NbPI. The genes were ligated to pCV-LIC-nYFP-C and pCV-LIC-cYFP-C (with yellow fluorescent protein [YFP] as the C-terminal fusion protein added), and pCV-NbPI-nYFP and pCV-P25-cYFP were constructed. Plasmids pCV-GUS-cYFP were as previously described (Fang et al. 2024). Confocal fluorescence observation and subcellular localisation analysis were conducted using pCV-LIC-GFP (C-terminal green fluorescent protein) and pCV-LIC-RFP (C-terminal red fluorescent protein), and pCV-P25-GFP and pCV-NbPI-RFP were constructed. To achieve the transient expression of proteins with C-terminal Myc tags in plants, the recombinant plasmid pCV-NbPI-Myc was constructed using the pCV-LIC-Myc vector carrying a C-terminal Myc protein tag. All the constructed vectors were validated by DNA sequencing.

4.3 | VIGS

To conduct VIGS experiments, the tobacco rattle virus (TRV) vector was introduced into *A. tumefaciens* GV3101 (Liu et al. 2002). Agrobacteria carrying vectors derived from TRV1 or TRV2 were resuspended in infiltration buffer (10 mM $MgCl_2$, 10 mM MES, 200 mM acetosyringone) and mixed in a 1:1 ratio. After incubation at room temperature for 3 h, the mixed culture was infiltrated into *N. benthamiana* plants at the six-leaf stage. The silencing phenotype appeared in the upper leaves 10 days post-infiltration.

4.4 | Yeast Two-Hybrid Experiments

The pGBK-P25 and pGAD-NbPI vectors were transformed into *Saccharomyces cerevisiae* Y2HGold. After transformation, cells were inoculated into SD/–Leu–Trp medium (a synthetic glucose-based medium without leucine and tryptophan) to verify the successful co-transformation of the two and then diluted in a concentration gradient into SD/–Leu–Trp–His–Ade medium (a synthetic glucose-based medium without leucine, tryptophan, adenine, and histidine) to verify the protein–protein interactions.

4.5 | BiFC

The plasmids pCV-NbPI-nYFP and pCV-P25-cYFP were introduced into different regions of *N. benthamiana* leaves by *Agrobacterium* infiltration, with pCV-GUS-cYFP as the control. The OD_{600} value of *Agrobacterium* was 0.05. The YFP fluorescence was observed by confocal microscopy at 2 days post-infiltration.

4.6 | Co-Immunoprecipitation Assay

The examined genes were fused with a GFP or Myc tag and agroinfiltrated into *N. benthamiana* leaves. At 2 days post-infiltration, proteins were extracted from leaf samples (eight discs) in cold GTEN extraction buffer (10% glycerol, 25 mM Tris–HCl, pH 7.5, 1 mM EDTA, 150 mM NaCl), 10 mM dithiothreitol, 1 mM phenylmethylsulfonyl fluoride (PMSF), 0.15% Nonidet P40, and 1× protease inhibitor cocktail (Roche). Subsequently, the leaf lysate was mixed with GFP-Trap magnetic beads (ChromoTek), thoroughly shaken, and then incubated gently at 4°C for 2 h. The beads were collected using a magnet and washed nine times with washing buffer (GTEN buffer containing 1 mM PMSF and 1× protease inhibitor cocktail, freshly prepared). The bound complexes were eluted by boiling in protein loading buffer for 10 min and then separated by SDS-PAGE on a 12% polyacrylamide gel and detected with anti-Myc and anti-GFP antibodies.

4.7 | Western Blotting

Total proteins of plants were extracted with lysis buffer (100 mM Tris–HCl, pH 8.8, 60% SDS, 2% β-mercaptoethanol). Proteins were separated in a 12% SDS-PAGE gel, transferred onto polyvinylidene fluoride (Millipore) by wet electroblotting, and detected with primary antibody and anti-mouse or -rabbit (TransGen) secondary antibody. The antigen–antibody complexes were visualised using Immoblion Western Chemiluminescent HRP Substrate (Millipore) under standard conditions. The large subunit of RuBisCO protein served as the loading control. Quantitative analysis of the western blot digital images was performed using ImageJ software.

4.8 | RNA Extraction and RT-qPCR

Total RNA was extracted with TRIzol according to the manufacturer's instructions (Invitrogen). The first-strand cDNA was synthesised using the TransScript All-in-One First-Strand cDNA Synthesis SuperMix with gDNA remover kit (TransGen). The expression levels of NbPI in NbPIOE, the expression level of PVX CP after infection, and the silencing efficiency of NbPI were detected by RT-qPCR using the primers listed in Table S1. qPCR was performed on a QuantStudio Real-Time Fluorescence Quantitative PCR System (Thermo Fisher Scientific) using the SYBR Green PCR Master Mix Kit (Vazyme), and data were analysed by the $2^{-\Delta\Delta C}_{t}$ method (Livak and Schmittgen 2001). The specificity of the qPCR primers was verified by pooled cDNA samples (melting curve). *Actin II* of *N. benthamiana* was selected as an internal reference gene (Fang et al. 2024).

4.9 | Confocal Microscopy

The agroinfiltrated leaf tissues of *N. benthamiana* were observed at 48–72 h post-agroinfiltration on an A1R HD25 confocal microscope (Nikon). Fluorescence signals (excitation/emission wavelength) for GFP (488/496–518 nm), YFP (514/529–550 nm) and mRFP (543/593–636 nm) were detected. Sequential scanning was used to avoid any interference between fluorescence channels.

4.10 | Data Analysis

Statistical graphs were generated using GraphPad Prism (v. 9.0) software. Data are presented as means ± *SD*, and statistical significance was analysed by Student's *t* test. At least three independent experiments (each with five biological or three technical repeats) were applied unless otherwise noted. ImageJ was

used to quantify average integrated density values of bands on immunoblots.

4.11 | Chemical Treatments

A total of 100 μM cycloheximide (Sigma) and water as a control were infiltrated into the leaves that had been pre-agroinfiltrated with targeted proteins to inhibit protein biosynthesis. A total of 10 mM 3-methyladenine (Sigma), 100 μM *Z*-Leu-Leu-Leu-al (MG132; Sigma), or an equal volume of dimethyl sulphoxide or water as control was used to inhibit the autophagy and 26S proteasome, respectively, as previously described.

Acknowledgements

We thank Professor M.J. Adams (Minehead, UK) for manuscript correction. This work was financially supported by the National Natural Science Foundation of China (32270144), State Key Laboratory for Managing Biotic and Chemical Threats to the Quality and Safety of Agro-products (2021DG700024-KF202425), the Natural Science Foundation of Ningbo City (2022J069), the Natural Science Foundation of Zhejiang Province (LY22C140001) and the K.C. Wong Magna Fund in Ningbo University.

Conflicts of Interest

The authors declare no conflicts of interest.

Data Availability Statement

The data that supports the findings of this study are available in the Supporting Information of this article.

References

Atabekov, J., E. Dobrov, O. Karpova, and N. Rodionova. 2007. "Potato Virus X: Structure, Disassembly and Reconstitution." *Molecular Plant Pathology* 8: 667–675.

Baulcombe, D. 2002. "Viral Suppression of Systemic Silencing." *Trends in Microbiology* 10: 306–308.

Bayne, E. H., D. V. Rakitina, S. Y. Morozov, and D. C. Baulcombe. 2005. "Cell-To-Cell Movement of Potato Potexvirus X Is Dependent on Suppression of RNA Silencing." *Plant Journal* 44: 471–482.

Chiu, M. H., I. H. Chen, D. C. Baulcombe, and C. H. Tsai. 2010. "The Silencing Suppressor P25 of Potato Virus X Interacts With Argonaute1 and Mediates Its Degradation Through the Proteasome Pathway." *Molecular Plant Pathology* 11: 641–649.

Diaz-Pendon, J. A., F. Li, W. X. Li, and S. W. Ding. 2007. "Suppression of Antiviral Silencing by Cucumber Mosaic Virus 2b Protein in *Arabidopsis* Is Associated With Drastically Reduced Accumulation of Three Classes of Viral Small Interfering RNAs." *Plant Cell* 19: 2053–2063.

Ding, S. W., H. Li, R. Lu, F. Li, and W. X. Li. 2004. "RNA Silencing: A Conserved Antiviral Immunity of Plants and Animals." *Virus Research* 102: 109–115.

Duan, C. G., Y. Y. Fang, B. J. Zhou, et al. 2012. "Suppression of *Arabidopsis* ARGONAUTE1-Mediated Slicing, Transgene-Induced RNA Silencing, and DNA Methylation by Distinct Domains of the Cucumber Mosaic Virus 2b Protein." *Plant Cell* 24: 259–274.

Fang, X., Z. Jia, T. Yu, et al. 2024. "FATTY ACID DESATURASE4 Enhances Plant RNA Virus Replication and Undergoes Host Vacuolar ATPase-Mediated Degradation." *Plant Physiology* 196: 1502–1517.

Grudkowska, M., and B. Zagdańska. 2004. "Multifunctional Role of Plant Cysteine Proteinases." *Acta Biochimica Polonica* 51: 609–624.

Gutierrez-Campos, R., J. A. Torres-Acosta, L. J. Saucedo-Arias, and M. A. Gomez-Lim. 1999. "The Use of Cysteine Proteinase Inhibitors to Engineer Resistance Against Potyviruses in Transgenic Tobacco Plants." *Nature Biotechnology* 17: 1223–1226.

Haxim, Y., A. Ismayil, Q. Jia, et al. 2017. "Autophagy Functions as an Antiviral Mechanism Against Geminiviruses in Plants." *eLife* 6: e23897.

Horsch, R. B., J. E. Fry, N. L. Hoffmann, et al. 1985. "A Simple and General Method for Transferring Genes Into Plants." *Science Adviser* 227: 1229–1231.

Jiang, L., Y. Lu, X. Zheng, et al. 2021. "The Plant Protein NbP3IP Directs Degradation of Rice Stripe Virus p3 Silencing Suppressor Protein to Limit Virus Infection Through Interaction With the Autophagy-Related Protein NbATG8." *New Phytologist* 229: 1036–1051.

Jiang, L., X. Zheng, Y. Liu, J. Chen, Y. Lu, and F. Yan. 2021. "Plant Protein P3IP Participates in the Regulation of Autophagy in *Nicotiana benthamiana*." *Plant Signaling & Behavior* 16: 1861768.

Kim, J. Y., S. C. Park, M. H. Kim, H. T. Lim, Y. Park, and K. S. Hahm. 2005. "Antimicrobial Activity Studies on a Trypsin-Chymotrypsin Protease Inhibitor Obtained From Potato." *Biochemical and Biophysical Research Communications* 330: 921–927.

Kim, M. H., S. C. Park, J. Y. Kim, et al. 2006. "Purification and Characterization of a Heat-Stable Serine Protease Inhibitor From the Tubers of New Potato Variety "Golden Valley"." *Biochemical and Biophysical Research Communications* 346: 681–686.

Lakatos, L., T. Csorba, V. Pantaleo, et al. 2006. "Small RNA Binding Is a Common Strategy to Suppress RNA Silencing by Several Viral Suppressors." *EMBO Journal* 25: 2768–2780.

Leshchiner, A. D., A. G. Solovyev, S. Y. Morozov, and N. O. Kalinina. 2006. "A Minimal Region in the NTPase/Helicase Domain of the TGBp1 Plant Virus Movement Protein Is Responsible for ATPase Activity and Cooperative RNA Binding." *Journal of General Virology* 87: 3087–3095.

Li, Y., Q. Sun, T. Zhao, et al. 2019. "Interaction Between Brassica Yellows Virus Silencing Suppressor P0 and Plant SKP1 Facilitates Stability of P0 In Vivo Against Degradation by Proteasome and Autophagy Pathways." *New Phytologist* 222: 1458–1473.

Lin, C. W., M. H. Su, Y. T. Lin, C. H. Chung, and H. M. Ku. 2015. "Functional Characterization of *Cucumis metuliferus* Proteinase Inhibitor Gene (*CmSPI*) in Potyviruses Resistance." *Viruses* 7: 3816–3834.

Liu, Y., M. Schiff, and S. P. Dinesh-Kumar. 2002. "Virus-Induced Gene Silencing in Tomato." *Plant Journal* 31: 777–786.

Livak, K. J., and T. D. Schmittgen. 2001. "Analysis of Relative Gene Expression Data Using Real-Time Quantitative PCR and the $2^{-\Delta\Delta C(T)}$ Method." *Methods* 25: 402–408.

Lu, Y., F. Yan, W. Guo, et al. 2011. "Garlic Virus X 11-kDa Protein Granules Move Within the Cytoplasm and Traffic a Host Protein Normally Found in the Nucleolus." *Molecular Plant Pathology* 12: 666–676.

Marshall, R. S., F. Li, D. C. Gemperline, A. J. Book, and R. D. Vierstra. 2021. "Autophagic Degradation of the 26S Proteasome Is Mediated by the Dual ATG8/Ubiquitin Receptor RPN10 in *Arabidopsis*." *Molecular Cell* 81: 2053.

Mitsumori, C., K. Yamagishi, K. Fujino, and Y. Kikuta. 1994. "Detection of Immunologically Related Kunitz and Bowman–Birk Proteinase Inhibitors Expressed During Potato Tuber Development." *Plant Molecular Biology* 26: 961–969.

Osmani, Z., M. S. Sabet, and K. S. Nakahara. 2022. "Aspartic Protease Inhibitor Enhances Resistance to Potato Virus Y and A in Transgenic Potato Plants." *BMC Plant Biology* 22: 241.

Premachandran, K., T. S. Srinivasan, and C. R. Wilson Alphonse. 2021. "In Silico Approach on Sequential and Structural Variability in Oryzacystatin and Its Interaction With Cysteine Protease Enzymes of Insect." *Phytochemistry* 186: 112728.

Qu, F., and T. J. Morris. 2005. "Suppressors of RNA Silencing Encoded by Plant Viruses and Their Role in Viral Infections." *FEBS Letters* 579: 5958–5964.

Raffeiner, M., S. Zhu, M. González-Fuente, and S. Üstün. 2023. "Interplay Between Autophagy and Proteasome During Protein Turnover." *Trends in Plant Science* 28: 698–714.

Sawano, Y., K. Hatano, T. Miyakawa, et al. 2008. "Proteinase Inhibitor From Ginkgo Seeds Is a Member of the Plant Nonspecific Lipid Transfer Protein Gene Family." *Plant Physiology* 146: 1909–1919.

Sels, J., J. Mathys, B. M. De Coninck, B. P. Cammue, and M. F. De Bolle. 2008. "Plant Pathogenesis-Related (PR) Proteins: A Focus on PR Peptides." *Plant Physiology and Biochemistry* 46: 941–950.

Sin, S. F., E. C. Yeung, and M. L. Chye. 2006. "Downregulation of *Solanum americanum* Genes Encoding Proteinase Inhibitor II Causes Defective Seed Development." *Plant Journal* 45: 58–70.

Tamayo, M. C., M. Rufat, J. M. Bravo, and B. San Segundo. 2000. "Accumulation of a Maize Proteinase Inhibitor in Response to Wounding and Insect Feeding, and Characterization of Its Activity Toward Digestive Proteinases of *Spodoptera littoralis* Larvae." *Planta* 211: 62–71.

Tilsner, J., O. Linnik, K. M. Wright, et al. 2012. "The TGB1 Movement Protein of Potato Virus X Reorganizes Actin and Endomembranes Into the X-Body, a Viral Replication Factory." *Plant Physiology* 158: 1359–1370.

Tsybina, T. A., Y. E. Dunaevsky, A. K. Musolyamov, T. A. Egorov, and M. A. Belozersky. 2001. "Cationic Inhibitors of Serine Proteinases From Buckwheat Seeds." *Biochemistry* 66: 941–947.

Varshavsky, A. 2017. "The Ubiquitin System, Autophagy, and Regulated Protein Degradation." *Annual Review of Biochemistry* 86: 123–128.

Velásquez, A. C., S. Chakravarthy, and G. B. Martin. 2009. "Virus-Induced Gene Silencing (VIGS) in *Nicotiana benthamiana* and Tomato." *Journal of Visualized Experiments* 2009: 1292.

Verchot, J. 2022. "Potato Virus X: A Global Potato-Infecting Virus and Type Member of the *Potexvirus* Genus." *Molecular Plant Pathology* 23: 315–320.

Verchot-Lubicz, J., C. M. Ye, and D. Bamunusinghe. 2007. "Molecular Biology of Potexviruses: Recent Advances." *Journal of General Virology* 88: 1643–1655.

Vogel, F., D. Hofius, and U. Sonnewald. 2007. "Intracellular Trafficking of Potato Leafroll Virus Movement Protein in Transgenic *Arabidopsis*." *Traffic* 8: 1205–1214.

Voinnet, O. 2001. "RNA Silencing as a Plant Immune System Against Viruses." *Trends in Genetics* 17: 449–459.

Voinnet, O., C. Lederer, and D. C. Baulcombe. 2000. "A Viral Movement Protein Prevents Spread of the Gene Silencing Signal in *Nicotiana benthamiana*." *Cell* 103: 157–167.

Wang, M. B., and M. Metzlaff. 2005. "RNA Silencing and Antiviral Defence in Plants." *Current Opinion in Plant Biology* 8: 216–222.

Wendrich, J. R., C. Y. Liao, W. A. van den Berg, B. De Rybel, and D. Weijers. 2015. "Ligation-Independent Cloning for Plant Research." *Methods in Molecular Biology* 1284: 421–431.

Wu, X., J. Liu, M. Chai, et al. 2019. "The Potato Virus X TGBp2 Protein Plays Dual Functional Roles in Viral Replication and Movement." *Journal of Virology* 93: e0163518.

Yang, X., Y. Lu, F. Wang, et al. 2020. "Involvement of the Chloroplast Gene Ferredoxin 1 in Multiple Responses of *Nicotiana benthamiana* to Potato Virus X Infection." *Journal of Experimental Botany* 71: 2142–2156.

Yang, X., Y. Tian, X. Zhao, et al. 2020. "NbALY916 Is Involved in Potato Virus X P25-Triggered Cell Death in *Nicotiana benthamiana*." *Molecular Plant Pathology* 21: 1495–1501.

Yu, P., and Z. Hua. 2023. "To Kill or to be Killed: How Does the Battle Between the UPS and Autophagy Maintain the Intracellular Homeostasis in Eukaryotes?" *International Journal of Molecular Sciences* 24: 2221.

Zhu, Q., A. Ahmad, C. Shi, et al. 2024. "Protein Arginine Methyltransferase 6 Mediates Antiviral Immunity in Plants." *Cell Host & Microbe* 32: 1566–1578.e5.

Zhu-Salzman, K., and R. Zeng. 2015. "Insect Response to Plant Defensive Protease Inhibitors." *Annual Review of Entomology* 60: 233–252.

Supporting Information

Additional supporting information can be found online in the Supporting Information section.